

Investigation of the Focal Spot Drift in Industrial Cone-beam X-ray Computed Tomography

Nadia FLAY^{1,3}, Wenjuan SUN¹, Stephen BROWN¹, Richard LEACH²,
Thomas BLUMENSATH³

¹Engineering Measurement Division, National Physical Laboratory, TW11 0LW, UK,

Tel: +44 208 943 6349; email: nadia.flay@npl.co.uk, wenjuan.sun@npl.co.uk, stephen.brown@npl.co.uk

²Department of Mechanical, Materials and Manufacturing Engineering, University of Nottingham, NG7 2RD, UK; email: Richard.Leach@nottingham.ac.uk

³Engineering Materials Group, Faculty of Engineering and the Environment, University of Southampton, SO17 1BJ, UK; Thomas.Blumensath@soton.ac.uk

Abstract. A study of the focal spot drift in an X-ray computed tomography system was conducted over a period of several months. In an attempt to eliminate additional unwanted sources of motion within the X-ray computed tomography system, a novel sample design was implemented. The focal spot drift was measured in scans with different starting X-ray tube temperatures, with the X-ray tube power kept below 6 W. The presence of drift was detected in all scans. The magnitude of the drift varied depending on the experimental settings but did not exceed 0.5 of a pixel in the image plane over a period of 10 000 s. The results from these drift experiments were then compared to results in which the sample was affected by the instabilities of the structure containing the rotation stage. It was found that the contribution to the total drift in 2D projections due to the instability of the structure containing the rotation stage is greater than the contribution from the focal spot drift. Some of the main issues associated with measurement of the focal spot drift are discussed and further possibilities for research are proposed.

Keywords: XCT, focal spot drift.

1. Introduction

Different aspects of the focal spot, such as its size, shape, positional stability, intensity and energy distribution across the focal spot area, have a direct impact on the quality of the X-ray computed tomography (XCT) images. For example, regular operation of the X-ray tube results in an increase in tube temperature, this temperature increase causes a change in the geometry of the X-ray tube, which can manifest itself as a ‘drift’ of the focal spot. Such a drift leads to instability in the imaging geometry, thereby introducing errors in the image reconstruction process and affecting the accuracy of dimensional measurements [1].

The influence of focal spot drift on the positional stability of 2D projections has been investigated experimentally, as well as using computer simulation techniques [2]–[8]. Most experimental methods consist of observing the drift in the 2D projections of a stationary reference object over a period of time. Reference objects used in the literature include a small metal sphere [2], calibrated ruby spheres [7], a calibrated hole plate [3] and a cross wire [8], [9]. Specific features of the reference object are determined in each projection and the change in position of the feature between images is calculated. In literature, the observed positional changes of the feature are often automatically attributed to the drift of the focal spot. It is important to mention, however, that other factors, such as the mechanical rigidity of the X-ray tube-object-detector assembly, variations in the X-ray flux and electronic properties of the detector can all influence the overall stability of the 2D projections. Understanding how much each factor contributes to the overall drift in 2D projections can be problematic. It has been observed that even for the same X-ray system, different experimental arrangements can produce different values of the overall drift. A different approach for measuring the focal spot drift is described in [9]. Here, the focal spot drift was derived from the length extension of the X-ray tube which was measured using a micrometer gauge.

Although the aforementioned investigations provide an estimate for the magnitude of the focal spot drift, it was difficult to perform a comparison of the results. The difficulty was, in part, due to the fact that the studies were carried out using different XCT systems with a variety of experimental set-ups. The comparison was complicated further by the differences in the way the focal spot drift data was presented and interpreted. Despite these difficulties, a few conclusions about focal spot drift can be drawn from the previous investigations: a) a shift in the position of a reference object in 2D projections was evident in all reported experiments; b) the largest shift in 2D projections was observed in the first few minutes of the experiment, corresponding to the largest focal spot drift due to rising temperatures inside the X-ray tube; c) increasing the power of the X-ray tube increases the magnitude of the focal spot drift [7]. One study reported a repeatable nature of the focal spot drift, where the focal spot drift was identified as the main contributor to the positional instability of 2D projections [3]. Another study found the drift to be linear with superimposed sinusoidal oscillations [2].

The purpose of this present study was to conduct an investigation of the focal spot drift and its correlation with thermal behaviour of an XCT system. The novel experimental set-up and the reference objects were designed in such a way as to minimise the number of factors that can influence the positional stability of 2D projections. The experiments were performed with different starting temperature of the X-ray tube. The focal spot drift was calculated in both the x and the y axes. The long term stability of the system and the repeatability of the experiments were assessed for tube power below 6 W. The results from the experiments were then compared to the results of the scan in which the reference object was affected by the motion of the rotation stage. This paper is organised in the following way: the technical specification of the XCT system and the experimental set-up are described in section 2. The results from monitoring the focal spot drift and the temperature fluctuations are discussed in section 3. The summary and conclusions are presented in section 4.

2. XCT system, Materials and Experimental setup

2.1 XCT System

The system used in this study was a Nikon Metrology XT H 225 M [10]. One distinct feature of this XCT system is that the target part of the X-ray gun is mounted into a metal bracket which is firmly attached to the metal frame inside the chamber. Such design allows the source-to-detector distance to remain largely unaffected as the tube undergoes thermal expansion during scanning. The manufacturer's specification of the system is shown in table 1.

Table 1. XT H 225 M System Manufacturer's Specification.

Dimensions:	
Source-to-detector distance	1180 mm (nominal)
Enclosure temperature	19 °C to 21 °C
X-ray source:	
Type	Nikon Metrology 225 kV open tube
Operating voltage	25 kV to 225 kV
Beam current	0 mA to 2 mA
Target material	tungsten, molybdenum, silver, copper
Target type	reflection
Detector:	
Type	PerkinElmer XRD 1620 AN3 CS
Active pixels	2 000 × 2 000, with 200 µm pitch

The tungsten part of the multi-target was used during these experiments.

2.2 Materials and Experimental Setup

2.2.1 Environmental Conditions and Temperature Recordings

The XCT system was located in an air-conditioned laboratory with the temperature controlled to $20.0\text{ }^{\circ}\text{C} \pm 0.1\text{ }^{\circ}\text{C}$ and relative humidity of $45\% \pm 5\%$. The system is fitted with an internal cooling system which is specified to maintain the temperature inside the chamber at $20.0\text{ }^{\circ}\text{C} \pm 1.0\text{ }^{\circ}\text{C}$. In order to record temperature fluctuations during the experiments, an Edale CD1.1 thermometer with three disc thermistors for measuring surface temperature was used. The resolution of the thermometer is $\pm 0.01\text{ }^{\circ}\text{C}$. Sensor 1 was placed on the metal part of the X-ray tube just above the target. Sensor 2 was attached to the water pipe below the target and Sensor 3 was attached to the filter mount adjacent to the sample (figure 2). Temperature readings from each sensor were taken every 8 s.

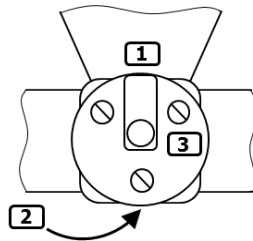


Figure 1. Positions of three thermal sensors on the X-ray tube: sensor 1 is attached to the lower part of the tube, sensor 2 is attached to the water pipe underneath the target, sensor 3 is attached to the filter holder next to the sample.

2.2.2 Sample Design

Given the difficulties that exist in isolating the focal spot drift from other factors contributing to the instabilities in 2D projections, two samples were designed. Both samples were small metal spheres surrounded by transparent materials. Sample 1 was a steel ball of 0.79 mm diameter embedded in the centre of a polyurethane cylinder of 10 mm diameter and 5.42 mm height (figure 2a). Sample 2 was a steel ball of 0.79 mm diameter attached to a borosilicate glass plate of 1 mm thickness (figure 2b). The nominal thermal expansion coefficient of polyurethane is $57.6 \times 10^{-6}\text{ K}^{-1}$, of steel is $13 \times 10^{-6}\text{ K}^{-1}$ and that of borosilicate is $3.3 \times 10^{-6}\text{ K}^{-1}$. Such sample design offered several advantages in observing the drift of the focal spot. Firstly, the ability to place the samples directly into the filter holder, which is attached to the opening of the X-ray tube, allowed the elimination of the structure containing the rotation stage as an additional source of mechanical instability. Secondly, such close proximity to the opening of the X-ray tube maximises the magnification, thus improving the sensitivity in the observed focal spot drift. The magnification factor, m (quotient of source-to-detector distance to source-to-object distance) was approximately 128 for sample 1 and 130 for sample 2. Embedding a steel ball into transparent material offers yet another advantage. Since steel absorbs more X-rays than polyurethane or borosilicate, sharp 2D images of a sphere can be produced, allowing more accurate edge detection during image processing. Due to some absorption of softer X-rays by the transparent material, the uniformity of the background in 2D projections over the scan duration is also improved.

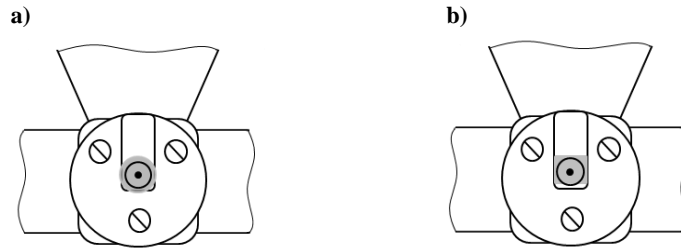


Figure 2. a) Sample 1 fitted in the filter holder; b) sample 2 fitted in the filter holder.

2.2.3 Image Acquisition

To analyse the focal spot drift in the Nikon Metrology XT H 225 M, thirty-eight scans were acquired over a three month period. During this time the filament was changed twice. The X-ray tube was operated at power below 6 W. Image acquisition settings were at one frame per second, with one frame per projection. In all experiments the samples were placed in the holder for at least two hours before being scanned, to minimise motion due to the settling of the sample. In accordance with the manufacturer's instructions, the XCT system remained switched on even when no X-rays were produced. To assess the influence of the X-ray tube temperature experiments were performed in two modes: cold and hot.

Cold mode

- no X-rays were generated before the start of the scan,
- each scan comprises 3142 projections (optimal number of projections for these settings),
- eighteen cold scans were acquired.

Hot mode

- the X-rays were switched on for at least twenty minutes prior to the scan,
- each scan comprises 10 000 projections (maximum number of projections),
- eighteen hot scans were acquired.

To evaluate the behaviour of the focal spot over a much longer period of time, two additional scans lasting over eleven hours were performed. Such scan duration was achieved by setting the maximum number of projections to 10 000 and adjusting the image acquisition settings to four frames per projection (at one frame per second).

2.2.4 Image analysis

After completing each scan, all 2D projections were analysed in Matlab using the procedure similar to the one described in [2]. Images of the steel ball (sphere) were first cropped (figure 3a), then the edge of the sphere was detected using the Canny edge detection algorithm with customised threshold parameters (figure 3b) [11]. The (x,y) coordinates of the edge were traced, and a circle was fitted to these coordinates using a non-linear least squares circle fitting algorithm. The x and y coordinates of the centre of the fitted circle were then determined. To calculate the shift in the (x,y) coordinates of the centre of the fitted circle throughout the whole scan, the (x,y) centre coordinates in the first image were subtracted from the (x,y) centre coordinates in all subsequent images. The focal spot drift was calculated by combining the data

of the shift in the (x,y) centre coordinates and the magnification factor. This procedure was repeated for all cold and hot scans.

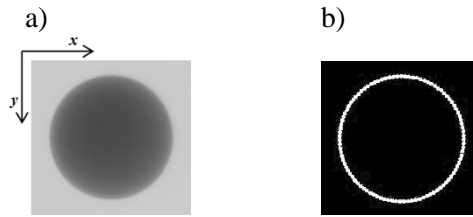


Figure 3. Image processing: a) a cropped image of the steel ball and b) circle fitted to the traced boundary.

3. Results and Discussion

3.1 Cold Scans

3.1.1 Analysis of Temperature Data

Eighteen cold scans were acquired over a period of three months. Figure 4 shows a temperature log of the sensors 1, 2 and 3 of a typical cold scan (scan A). From the moment the X-rays were switched on, the temperature sensor attached to the lower part of the tube, sensor 1, showed a steady increase in temperature of around 0.2 °C during the initial eight minutes of the scan. Thereafter the temperature stabilised, varying within less than 0.05 °C throughout the scan. The sensor attached to the water pipe, sensor 2, recorded a stable temperature irrespective of whether the X-rays were switched on or off. The readings were fluctuating within 0.06 °C throughout the experiment.

Sensor 3, which was attached to the filter holder adjacent to the sample, recorded a more rapid and of greater magnitude increase in temperature. Here, temperature increased by almost 0.9 °C within the first four minutes, thereafter it stabilised and continued to fluctuate within 0.05 °C. Since sensor 3 was placed close to the sample, it can be inferred that in the first few minutes, the sample underwent a similar temperature increase as that of sensor 3. There is a time delay between the production of X-rays at the start of the scan and the acquisition of the first image. This delay varies from several seconds to several minutes depending on scan settings. For scan A, which represents a standard industrial scan, this delay was around 30 s. During this time sensor 3 recorded a rise in temperature of over 0.5 °C, which is more than half of its total increase. This delay allows to minimise the potential shift in the (x,y) centre coordinates due to thermal expansion of the sample. At the start of each scan, sensor 1 displayed approximately 1 °C higher temperature than sensors 2 and 3. This is due to the fact that sensor 1 was attached to the lower part of the gun where the focus coil, which is constantly energised, is located.

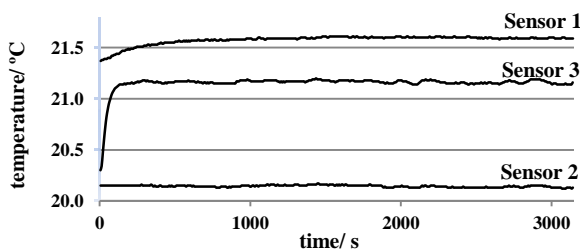


Figure 4. Temperature log of the three sensors in scan A.

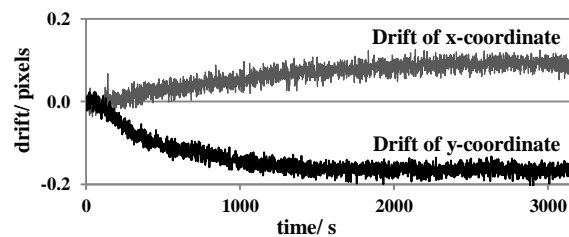


Figure 5. Drift in the (x,y) centre coordinates in scan A.

3.1.2 Analysis of the drift

Figure 5 shows the drift of the (x,y) coordinates of the centre of the fitted circle in a series of 2D projections acquired during scan A. It is essential to note that this drift is due to the combination of the relative motion between the focal spot, the sample and the detector; therefore, it is difficult to establish a direct correlation between observed drift and any individual components in the system. However, with the current experimental setup, it was reasonable to assume that the instabilities of the 2D projections were predominantly due to the drift of the focal spot. To calculate the drift of the focal spot, the sample was assumed to be stationary (potential motion due to thermal expansion of the sample is discussed below). The magnitude of the focal spot drift was calculated by multiplying the magnitude of the drift of 2D projections with the quotient of the source-to-object and object-to-detector distance.

In scan A, the total drift of the x-coordinate was around 0.1 pixels (20 μm) and the drift of the y-coordinate was just below 0.2 pixels (40 μm). At magnification of 130 and the detector pixel size of 200 μm , the corresponding drift of the focal spot in the x-axis was calculated to be around 0.15 μm , and in the y-axis was approximately 0.3 μm . Combining the information from the graphs in figures 4 and 5, there appears to be a close correlation between the rise in temperature recorded by the sensor attached to the lower part of the tube and the drift pattern of the (x,y) coordinates. This correlation supports the assumption that most of the recorded drift of the (x,y) coordinates in 2D projections is due to the drift of the focal spot rather than other factors, such as the motion due to thermal expansion of the sample. Another observation in support of this assumption is discussed below.

In most cold scans a slightly larger drift of the y-coordinate compared to the x-coordinate was observed, irrespective of whether sample 1 or sample 2 was used. The initial drift of the y-coordinate was predominantly negative; however, no such preferential direction of motion was seen in the x-axis. For sample 1, where the cylinder rests at the bottom of the filter holder, some of this preferential motion in the upward y-direction could perhaps be attributed to thermal expansion of the sample. However, taking into account the magnitude of the drift, the corresponding increase in temperature over the initial few minutes recorded by sensor 3, as well as the dimensions and materials of sample 1, the possible drift due to thermal expansion was calculated to be below 0.1 μm . This is less than a third of the observed drift. A similar drift of the (x,y) coordinates was observed in cold scans when using sample 2. Even though a slightly different design of sample 2 and the way it was mounted in the filter holder allowed it to be largely unaffected by motion due to thermal expansion. Based on the above observations, it can be concluded that the observed drift pattern is predominantly due to the instability of the focal spot as the temperature inside the X-ray gun begins to rise.

3.2 Hot Scans

3.2.1 Analysis of Temperature Data

Figure 6 shows the temperature log of a typical hot scan (scan B). Unlike cold scans, where a clear increase in temperature was recorded by sensor 1 and sensor 3, no such increase was observed in hot scans. The temperature fluctuations for all three sensors did not exceed 0.1 $^{\circ}\text{C}$ in any of the scans. These results confirm that switching the X-rays on for at least twenty minutes prior to the start of the scan, allows the XCT system to reach its thermal equilibrium, which is sustained throughout every experiment.

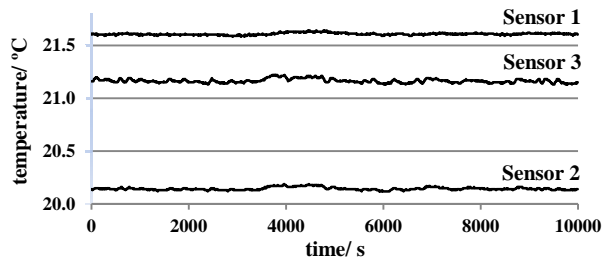


Figure 6. Temperature log of the three sensors in scan B.

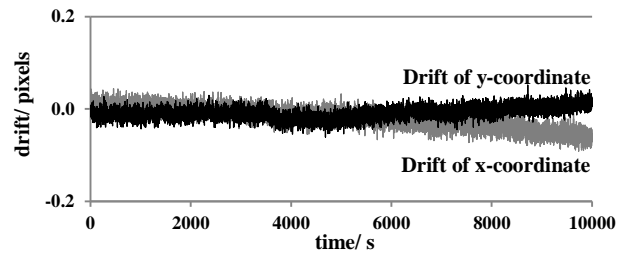


Figure 7. The drift in the (x,y) centre coordinates in scan B.

3.2.2 Analysis of the Drift

Figure 7 shows the drift of the (x,y) coordinates of the centre of the fitted circle in scan B. The drift of the x-coordinate was less than 0.07 pixels ($14\ \mu\text{m}$); at magnification of 130 it corresponds to approximately $0.1\ \mu\text{m}$ drift of the focal spot in the x-axis. The drift of the y-coordinate was around 0.02 pixels ($4\ \mu\text{m}$), corresponding to approximately $0.03\ \mu\text{m}$ drift of the focal spot in the y-axis. In all eighteen hot scans, lasting 10 000 s each (three times the length of a standard industrial scan), no drift of the (x,y) centre coordinates exceeded the magnitude of 0.1 pixels ($20\ \mu\text{m}$). This value corresponds to approximately $0.15\ \mu\text{m}$ drift of the focal spot in either axis. The results from the hot scans support the idea that most of the observed drift of the (x,y) centre coordinates is associated with increasing temperature in the X-ray tube.

3.3 Long Term Stability

3.3.1 Drift Analysis of the Eleven Hour Scan with Sample Placed into the Filter Holder

The purpose of the first long scan was to evaluate a long-term stability of the XCT system at power below 6 W. The long scan comprised 10 000 projections and lasted over eleven hours (scan C). Although this scan was performed in cold mode, due to the length of the experiment, the delay between the start of the scan when the X-rays were switched on and the time of the acquisition of the first projection was approximately ten minutes. Therefore, most of the temperature rise happened before the acquisition of the first image.

Just as in hot scans the temperature sensors recorded stable temperatures slightly fluctuating within $0.1\ ^\circ\text{C}$ throughout the scan. Despite the thermally stable conditions, a clear drift of the (x,y) centre coordinates was observed (figure 8). Over eleven hours a total drift of the x-coordinate was just over 0.4 pixels ($80\ \mu\text{m}$), corresponding to approximately $0.6\ \mu\text{m}$ drift of the focal spot in the x-axis. The drift of the y-coordinate was around 0.1 pixels ($20\ \mu\text{m}$), corresponding to $0.15\ \mu\text{m}$ drift of the focal spot in the y-axis. Based on these results, it can be inferred that the observed drift was not due to thermal conditions inside the X-ray tube. One possible explanation is that the drift is the result of the gradual change in the surface of the target due to its damage by the electron beam. Although some have shown that no visible wear of tungsten target was observed for X-ray tube power settings of below 8 W [12]. Another possibility is that the observed drift is caused by the relative movement in the X-ray tube, metal frame and detector assembly.

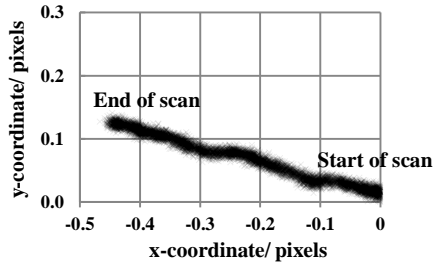


Figure 8. The drift of the (x,y) centre coordinates in scan C.

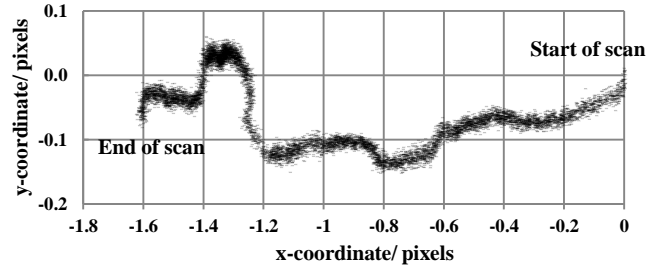


Figure 9. The drift of the (x,y) centre coordinates in scan D.

3.3.2 Drift analysis of the eleven hour scan with sample placed next to the rotation stage

The purpose of the second long scan (scan D) was to evaluate the long-term drift in 2D projections when the sample was mounted onto the mechanical structure containing the rotation stage. Sample 1 was fixed to the metal plate on the source side of the rotation stage, on the axis, so as to remain nominally stationary during the stage rotation associated with measurement. Due to the influences of the motion of the rotation stage, some parasitic motion of the sample was anticipated during measurement. Magnification in this experiment was around 61. All other experimental settings were identical to those of the previous long scan. As in scan C, the temperature fluctuations for all three sensors did not exceed 0.1 °C throughout the experiment. Figure 9 shows the drift of the (x,y) centre coordinates in scan D. Although scans C and D were acquired at different magnification, the comparison of data in figures 8 and 9 clearly demonstrates that the contribution to the total drift in 2D projections due to the instability of the structure containing the rotation stage is greater than the contribution from drift of the focal spot at tube power below 6 W.

4. Summary, Conclusions and Future Work

A study of the focal spot drift and its correlation with thermal behaviour of an XCT system was conducted over a period of several months. The thermal performance of the system is summarised in table 2. On the basis of these results, it can be concluded that the system demonstrated stable and repeatable thermal behaviour at the X-ray tube settings below or equal to 6 W. Further studies are needed to evaluate the thermal behaviour of the system at higher power settings.

Table 2. Temperature Data Summary.

Sensor label	Temperature before switching the X-rays on	Temperature at the end of the experiments
Sensor 1	21.38 °C ± 0.01 °C	21.60 °C ± 0.01 °C
Sensor 2	20.15 °C ± 0.03 °C	20.15 °C ± 0.03 °C
Sensor 3	20.30 °C ± 0.01 °C	21.20 °C ± 0.01 °C

In order to observe the drift of the focal spot in the XCT system, a novel experimental set-up and reference objects were designed in a way so as to minimise the number of factors that can influence the positional stability of 2D projections. The scans were performed in two modes: cold and hot. Each cold scan comprises 3142 projections, which is the optimal number of projections for these settings. Each hot scan comprises 10 000 projection, which is the maximum number of projections for these settings. Additionally, two 11 hour scans were performed in order to assess a long-term performance of the system, as well as to evaluate the

influence of the sample positioning on the acquired drift data. The following observations and conclusions were made:

- The presence of the focal spot drift was evident in all scans.
- For all cold scans acquired over a period of fifty-three minutes, the drift of the (x,y) centre coordinates in the x-axis did not exceed 0.15 pixels (30 μm), corresponding to approximately 0.25 μm drift of the focal spot. The drift in the y-axis did not exceed 0.4 pixels (80 μm), corresponding to approximately 0.6 μm drift of the focal spot.
- In cold scans most of the drift in both axes happened during the initial eight to ten minutes. The pattern of the drift was in close correlation with the pattern of temperature increase recorded by the sensor attached to the lower part of the X-ray tube. It can, therefore, be concluded that the observed drift is predominantly due to the instability of the focal spot as the temperature inside the X-ray tube begins to rise. Others have reported the drift pattern stabilising approximately two hours after switching on the X-ray tube [7]. Given such variations in the length of time it takes for different X-ray tubes to stabilise, it is advisable for the user to identify the behaviour of the focal spot drift that is characteristic to their particular X-ray system. It is then advised, whenever possible, to allow the X-ray tube to stabilise for an appropriate length of time prior to image acquisition.
- For all hot scans acquired over a period of around three hours, the magnitude of the drift of the (x,y) centre coordinates did not exceed 0.1 pixels (20 μm) in either axes, corresponding to approximately 0.15 μm drift of the focal spot. It is important to note that although hot scans comprised 10 000 projections, most industrial scans are performed using only 3 142 projections (optimal manufacturer's setting). This means that at the X-ray tube power below 6 W, the overall drift of the focal spot will not exceed 0.1 μm in either axis. Such small value of the drift is within the noise of the system.
- No general trend to the direction of the drift was observed in hot experiments. The start direction of the drift appeared to be random; however, once the direction was initiated, the drift continued in that direction. Unlike other studies, where the drift was found to be a repeatable phenomenon, these findings make even the notion of positional correction of 2D projections using previously known focal spot drift data impossible.
- The results from the 11 hour scan, with the sample placed in the filter holder, revealed a presence of a steady drift of the (x,y) centre coordinates throughout the duration of the scan despite stable temperature readings from all three sensors. It can, therefore, be inferred that the observed drift was not only due to thermal conditions inside the X-ray tube, but also the result of additional factors that require further investigation. One possible explanation is that the drift is the result of the gradual change of the surface of the target due to its damage by the electron beam. Another possibility is that the observed drift is caused by the relative movement in the X-ray tube, metal frame and detector assembly.
- Data acquired from the 11 hour scan, where the sample was placed onto the structure containing the rotation stage, shows a very different drift pattern of the (x,y) centre coordinates compared to all other cold and hot scans both in magnitude and direction. The result demonstrates that for this XCT system the contribution to the total drift in 2D projections due to the instability of the structure containing the rotation stage is greater than the contribution from the focal spot drift. The significance of this finding is twofold. Firstly, if the main objective is to investigate the drift of the focal spot in an XCT system, it is essential that the sample and the experimental set-up are designed in such a way as to eliminate as many additional sources of motion as possible. If not, drift data acquired from 2D projections can be wrongly attributed to the drift of the focal spot. Secondly, if the main objective is to correct for the positional instability of 2D projections using a reference object technique, it is important

that the reference object is mounted in such a way that during a scan it ‘follows the path’ of the object of interest as closely as possible. Otherwise, this process of correction itself may introduce errors into the reconstructed 3D volume. This is not a trivial task and requires an in-depth understanding of how various parts of the XCT system perform during different scanning conditions.

Acknowledgments

This work was funded by the BIS National Measurement System Engineering and Flow Metrology Programme. We also thank Dr James Claverley, Dr Andrew Henning, Dr Claudiu Giusca and Massimiliano Ferrucci (National Physical Laboratory) for their contributions.

References

- [1] Curry T S, Dowdey J E and Murr R E 1990 *Christensen's physics of diagnostic radiology* 4th edition (Lea & Febiger)
- [2] Hiller J, Maisl M and Reindl L M 2012 Physical characterization and performance evaluation of an X-ray micro-computed tomography system for dimensional metrology applications *Measurement Science and Technology* **23** 085404
- [3] Vogeler F, Verheecke W, Voet A and Kruth J 2011 Positional stability of 2D X-ray images for computer tomography International Symposium of Digital Industrial Radiology and Computed Tomography (Proceedings) MO33
- [4] Reisinger S, Schmitt M and Voland V 2012 Geometric adjustment methods to improve reconstruction quality on rotational cone-beam systems Website: <http://www.ndt.net/article/ctc2012/papers/279.pdf> Accessed in March 2014
- [5] Fröba T and Steffen J P 2011 Assessing the effect of focal spot movement on the accuracy of CT results by using a simulation technique Website: <http://www.ndt.net/article/ctc2012/papers/253.pdf> Accessed in March 2014
- [6] Steffen J P and Fröba T 2011 Reducing the focal spot shift of microfocus X-ray tubes to increase the accuracy of CT-based dimensional measurement Website: <http://www.ndt.net/article/dir2011/papers/mo11ab~1.pdf> Accessed in March 2014
- [7] Weiss D, Deffner A and Kuhn C 2010 Einfluß der Quellungsbewegung auf Reproduzierbarkeit und Antastabweichung im Röntgen-Computertomographen Website: <http://www.ndt.net/article/ctc2010/papers/227.pdf> Accessed in March 2014
- [8] Uhlman N, Salamon M, Burtzloff S, Porsch F, Johansson W, Nachtrab F and Hanke R 2008 Components and methods for highest resolution computed tomography Website: http://www.ndt.net/article/aero2008/aero08_M19_Uhlman_Norman.pdf Accessed in February 2014
- [9] Fröba T and Steffen J P 2011 The advancement of microfocus reflection tubes for industrial applications in measurement technology 50th Annual Conference of the British Institute of Non-Destructive Testing (Proceedings)
- [10] “MCT225 for Metrology CT: Absolute accuracy for inside geometry | Metrology CT | X-ray and CT Inspection | Products | Nikon Metrology.” [Online]. Available: [http://www.nikonmetrology.com/en_EU/Products/X-ray-and-CT-Inspection/Metrology-CT/MCT225-for-Metrology-CT-Absolute-accuracy-for-inside-geometry/\(specifications\)](http://www.nikonmetrology.com/en_EU/Products/X-ray-and-CT-Inspection/Metrology-CT/MCT225-for-Metrology-CT-Absolute-accuracy-for-inside-geometry/(specifications)) Accessed: 14-Oct-2014
- [11] Nixon M 2012 *Feature extraction & image processing for computer vision* 3rd edition (Academic Press)
- [12] Grider D E, Wright A and P K Ausburn 1986 Electron beam melting in microfocus X-ray tubes *J. Phys. D: Appl. Phys.* **19** 2281–2292